ELSEVIER

Biochimica et Biophysica Acta 1507 (2001) 180–193

BIOCHIMICA ET BIOPHYSICA ACTA

BBA

www.bba-direct.com

Review

Fourier transform infrared spectroscopy of primary electron donors in type I photosynthetic reaction centers

Jacques Breton *

SBE/DBCM, CEA-Saclay, 91191 Gif-sur-Yvette Cedex, France

Received 11 December 2000; received in revised form 12 April 2001; accepted 10 May 2001

Abstract

The vibrational properties of the primary electron donors (P) of type I photosynthetic reaction centers, as investigated by Fourier transform infrared (FTIR) difference spectroscopy in the last 15 years, are briefly reviewed. The results obtained on the microenvironment of the chlorophyll molecules in P700 of photosystem I and of the bacteriochlorophyll molecules in P840 of the green bacteria (*Chlorobium*) and in P798 of heliobacteria are presented and discussed with special attention to the bonding interactions with the protein of the carbonyl groups and of the central Mg atom of the pigments. The observation of broad electronic transitions in the mid-IR for the cationic state of all the primary donors investigated provides evidence for charge repartition over two (B)Chl molecules. In the green sulfur bacteria and the heliobacteria, the assignments proposed for the carbonyl groups of P and P^+ are still very tentative. In contrast, the axial ligands of P700 in photosystem I have been identified and the vibrational properties of the chlorophyll (Chl) molecules involved in P700, $P700^+$, and $^3P700$ are well described in terms of two molecules, denoted P_1 and P_2, with very different hydrogen bonding patterns. While P_1 has hydrogen bonds to both the 9-keto and the 10a-ester C=O groups and bears all the triplet character in $^3P700$, the carbonyl groups of P_2 are free from hydrogen bonding. The positive charge in $P700^+$ is shared between the two Chl molecules with a ratio ranging from 1:1 to 2:1, in favor of P_2, depending on the temperature and the species. The localization of the triplet in $^3P700$ and of the unpaired electron in $P700^+$ deduced from FTIR spectroscopy is in sharp contrast with that resulting from the analysis of the magnetic resonance experiments. However, the FTIR results are in excellent agreement with the most recent structural model derived from X-ray crystallography of photosystem I at 2.5 Å resolution that reveals the hydrogen bonds to the carbonyl groups of the Chl in P700 as well as the histidine ligands of the central Mg atoms predicted from the FTIR data.

Keywords: Photosynthesis; Photosystem I; Type I reaction center; Primary electron donor; Fourier transform infrared spectroscopy

1. Introduction

In a manner similar to what has occurred in the field of the reaction centers (RCs) of purple photosynthetic bacteria since about 1985, the availability of the X-ray structural model of PSI since about 1995 has raised a number of new questions which constitute an interesting challenge for the spectroscopists. On the one hand, the vast amount of pre-

Abbreviations: ADMR, absorbance detected magnetic resonance; BChl, bacteriochlorophyll; Chl, chlorophyll; ENDOR, electron nuclear double resonance; EPR, electron paramagnetic resonance; FeS, iron–sulfur clusters; F_A, F_B, F_X, FeS electron acceptors of PSI; FTIR, Fourier transform infrared; P, primary electron donor; PSI, photosystem I; RC, reaction center; THF, tetrahydrofuran; WT, wild-type

* Fax: +33-1-6908-8717.

E-mail address: cadara3@dsvidf.cea.fr (J. Breton).

0005-2728/01/$ – see front matter
PII: S0005-2728(01)00206-7

viously obtained spectroscopic data and the interpretations provided have to be confronted to the crystallographic structural information and a model consistent with the results of both approaches has to be presented. On the other hand, the possibility offered by several types of spectroscopy to probe the different electronic states of the cofactors involved in the functional act of photosynthetic charge separation, represents an important addition to the X-ray structural model of PSI [1,2], that has so far only probed the static neutral state of the RC. A combined analysis could be of great help to delineate the possible changes in structure that accompany the separation and stabilization of charges. In the specific case of PSI RCs, this is obviously a dynamic process in view of the improvements in the quality of the X-ray data and the refinement of the structural model.

Vibrational spectroscopy represents a valuable tool to investigate at a submolecular level both the photosynthetic cofactors and the protein, their interaction in the ground state, as well as the changes of these interactions and of the protein structure that are liable to occur in the charge separated states. In the case of type I photosynthetic RCs, the core polypeptides of which contain a large number of strongly bound antenna pigments, FTIR spectroscopy, and notably the light-induced difference version of this technique, seems well suited for such investigation. In the following, we will briefly review the results that have been gathered over the last 15 years using FTIR difference spectroscopy on the primary electron donors (P) involved in type I reactions, and discuss some of the most recent developments in the field.

2. FTIR spectroscopy of P700

2.1. Early studies

The initial investigation of the photooxidation of P700 by FTIR difference spectroscopy was performed in 1986 [3] very soon after the first light-induced FTIR difference spectra of a photosynthetic reaction, namely the photooxidation of the primary electron donor in chromatophores and RCs of purple photosynthetic bacteria, had been obtained at CEA/Saclay [4]. PSI particles isolated from pea and containing about 200 chlorophyll (Chl) molecules per P700 were lightly dried on a CaF_2 window in the presence of the artificial electron acceptor methyl viologen, rehydrated with Na ascorbate in Tris buffer, and covered with a second CaF_2 window to form a cuvette of a few μm thickness. High-quality FTIR difference spectra were recorded both under and following continuous illumination at 22°C [3]. In view of the rather unusual conditions used for preparing the FTIR sample, a kinetic control was performed on the same sample to follow the bleaching of the electronic absorption band of P700 at 706 nm and the appearance of the $P700^+$ cation band at 820 nm. The rationale for adding methyl viologen was to eliminate, or at least to strongly decrease, the contributions from the endogenous iron sulfur clusters (FeS), that are the PSI electron acceptors. However, when this artificial electron acceptor was omitted, the bands in the difference spectra were mostly unaffected, indicating that contributions from the reduction of the FeS centers F_A and F_B are small compared to those originating from the photooxidation of P700.

In the absence of FTIR spectra of isolated Chl_a^+, assignment of the spectral changes was mostly limited to the negative bands, i.e., those that pertain to the neutral Chl species for which IR bands have long been assigned. A large negative band at $\sim$1700 cm^{-1} was already recognized as a candidate for the 9-keto carbonyl of the Chl_a molecule(s) constituting P700 while the negative bands located at 1735 and 1749 cm^{-1} were tentatively assigned to Chl_a esters C=O groups [3]. $^1H/^2H$ exchange as well as global isotope labeling with ^{13}C or ^{15}N on PSI particles isolated from the cyanobacterium *Spirulina geitleri* were used in an attempt to discriminate C=O vibrations originating from the Chl from those of the protein [5]. Upon ^{13}C labeling several bands in the 1750–1650 region were observed to downshift by $\sim$40 cm^{-1} as expected for C=O vibrations. Furthermore, no effect of $^1H/^2H$ exchange was observed on the largest bands, consistent with their assignment to Chl_a vibrations. Only relatively small signals in the amide II region (around 1550 cm^{-1}) were affected by labeling with ^{15}N, indicating that the protein backbone is making only a small contribution to the IR changes. However, the limited S/N of the spectra did not allow the C=O vibrations from the Chl to be

clearly discriminated from those of the protein for the ^{15}N labeling and precluded the analysis of the effect of $^{1}H/^{2}H$ exchange on the bands of small amplitude.

2.2. Comparison with Chl model compounds

In order to assign and interpret the features observed in the light-induced FTIR spectra associated with the primary reactions of photosynthesis, the IR spectra of isolated Chl model compounds have to be investigated in both their neutral and ionized states. Thus, the cation radicals of Chl_a and pyroChl_a (Chl_a lacking the 10a-ester carbonyl) were generated electrochemically in a special cell suited for the visible and IR spectral ranges [5–9]. Using this approach, it was found that the 9-keto C=O of Chl_a in tetrahydrofuran (THF) upshifted from 1693 to 1718 cm^{-1} as observed in the cation-minus-neutral difference spectrum while that of pyroChl_a shifted from 1686 to 1712 cm^{-1}. Furthermore, the lack of an IR signal in the C=O ester region of the cation-minus-neutral difference spectrum for pyroChl_a showed that the differential feature observed at 1751(+) and 1738(−) cm^{-1} in the cation-minus-neutral difference spectrum of Chl_a was due entirely to the 10a-ester C=O with no substantial contribution from the 7c-ester C=O [8,9]. The striking similarity between the large differential signals at 1718/1698 and 1718/1693 cm^{-1} in the $P700^+/P700$ and Chl_a^+/Chl_a difference spectra (Fig. 1), respectively, led to the assignment of the former to the frequency upshift upon primary donor photooxidation of the 9-keto group(s) of the Chl_a molecule(s) constituting P700 [9]. The high frequency of the 9-keto group vibration in P700 indicates an absence of bonding interaction with the PSI protein. Although participation of a bound 7c-ester C=O or of buried carboxylic acid residues could not be strictly excluded, the two differential signal observed at 1754/1749 and 1742/1735 cm^{-1} in the $P700^+/P700$ FTIR difference spectrum were rather assigned to 10a-ester C=O groups in inequivalent environments. On the other hand, the absence of effect of $^{1}H/^{2}H$ exchange on the latter signals showed that protonated Asp or Glu residues were not involved.

Nabedryk et al. [9] noticed that the assignment of the 1718 cm^{-1} band observed in the IR spectrum of

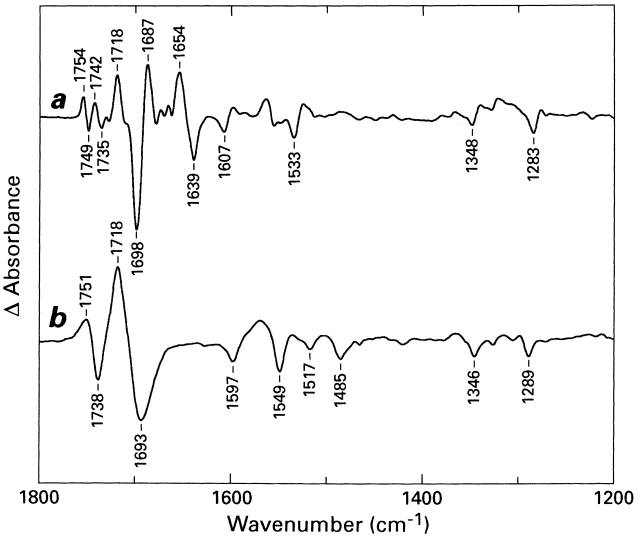

Fig. 1. (a) Light-induced $P700^+/P700$ FTIR difference spectrum of the photooxidation of a dry film of PSI particles from *Synechocystis* PCC 6803 at 5°C. (b) Redox-induced Chl_a^+/Chl_a FTIR difference spectrum of chlorophyll$_a$ cation formation at $U = +0.8$ V in deuterated tetrahydrofuran at 20°C. Peak-to-peak amplitudes are 2×10^{-3} and 6×10^{-2} absorbance units in a and b, respectively.

the radical cation of Chl_a in solution was at variance with that of a band at 1717 cm^{-1} in the resonance Raman spectrum of Chl_a^+ [10]. The latter was attributed to a downshifted 10a-ester C=O vibration consequent to the enolization of the 9-keto C=O after oxidation of Chl_a. The participation of enol forms of Chl_a in P700 photochemistry has been debated [11]. The observation in [9] that cation formation of isolated Chl_a induces the same frequency upshift (25–26 cm^{-1}) independently of the presence of the 10a-ester C=O provided compelling evidence for the absence of enolization upon Chl_a cation formation. Soon after, the same conclusion has also been reached from resonance Raman experiments on pyroChl_a^+ [12].

A light-induced $P700^+/P700$ FTIR difference spectrum from PSI particles from the cyanobacterium *Synechocystis* PCC 6803 has been reported [13]. This spectrum, which represented a control to estimate the effect of rather high levels of PSI contamination on the FTIR spectra of PSII reactions in a PSII-enriched preparation, compares well with the spectra previously reported on PSI preparations from various organisms [3,5,9,14].

Using a very different approach, namely that of

redox-induced FTIR difference spectroscopy, an investigation of the electrochemical oxidation of P700 in purified PSI preparations from *Synechocystis* PCC 6803 has been carried out [15]. In principle, this approach offers an advantage over the more common light-induced difference spectroscopy method insofar as possible contributions from the FeS centers should be eliminated. However, the early spectra were highly contaminated with contributions from antenna Chl_a molecules that exhibit reversible electrochemistry [15]. Careful developments of electrode modifications and mediator composition have resulted in a large improvement of the quality of the difference spectra, which become largely dominated by the $P700^+$/P700 contributions [16]. However, even in these improved spectra, several bands of small amplitude still appear conspicuously at the same positions as those of the Chl_a contaminants in the early spectra. Nevertheless, a comparison was made between a monomeric and a trimeric state of the PSI particles and small but significant differences were observed between 1640 and 1300 cm^{-1}. The effect of $^1H/^2H$ exchange was also investigated leading to the assignment of several of the bands to amide I and amide II vibrations [16].

A close resemblance between the FTIR difference spectra of the photoxidation of P700 and that of the primary electron donor in the HL(M202) heterodimer mutant of the purple photosynthetic bacterium *Rhodobacter sphaeroides* has been noticed [17]. In this mutant, the His residue at M202 which is the axial Mg ligand of one of the two bacteriochlorophyll (BChl) molecules that constitute the primary donor P870 in wild-type (WT) RCs is changed for a Leu residue. This prevents the ligation of a BChl and a bacteriopheophytin is inserted instead at the equivalent position. Upon photooxidation, the positive charge in the mutant is fully localized on the BChl half of the heterodimer. The similarity of the FTIR difference spectra was taken to suggest that in $P700^+$ the positive charge is localized on a single Chl_a molecule. Another observation was also indicative of a monomeric structure of $P700^+$, namely the absence in the P^+/P FTIR difference spectra of both the heterodimer mutant and of P700 of a specific mid-IR electronic transition characteristic of a dimeric structure of the oxidized special pair which had been previously predicted, observed around 2600 cm^{-1}, and analyzed in the spectra of WT RCs from several purple photosynthetic bacteria [18]. The apparent lack of such a band in the $P700^+$/P700 FTIR photo-induced difference spectrum was also noticed in the study of the redox-induced FTIR difference spectra [16]. More recently, the question of an electronic transition of $P700^+$ in the mid-IR has been reexamined after optimization of the detection conditions. Indeed such a transition, although relatively weak and peaking right under the region of intense absorption of the OH stretching vibration of liquid water at around 3300 cm^{-1}, has been unambiguously observed leading to a reinterpretation of the $P700^+$/P700 FTIR difference spectrum in terms of charge sharing over two Chl molecules in $P700^+$ [19].

2.3. Search for the axial ligands of P700

The X-ray crystal structure of PSI has revealed the existence of a twofold rotation axis joining the center of P700 to F_X and relating the eleven α-helices of the two subunits PsaA and PsaB [1]. The general organization of the cofactors forming two quasi-symmetric branches on their protein 'scaffold' is reminiscent of that encountered in the structure of the RC from purple photosynthetic bacteria where the core is constituted by the homologous L and M subunits. In the latter case, one of the main bonding interaction between the primary donor BChl and the protein is via liganding of homologous His residues to the central Mg atom. This has led to the idea that a search for conserved histidine side chains located at homologous positions in PsaA and PsaB, could help identify the axial ligands of the Chl of P700 [20,21]. After a systematic survey of such conserved residues, six pairs of His were targeted by site-directed mutagenesis and changed to pairs of Gln side chains in the green alga *Chlamydomonas reinhardtii*. A PSII-deficient background was used and purified thylakoids of the mutants were screened against WT samples for changes in the characteristics of P700 by several techniques, including FTIR difference spectroscopy [22]. The mutation of the His pair in helix 10 (PsaA–His676 and PsaB–His656) was the only one to result in a perturbed $P700^+$/P700 light-induced FTIR difference spectrum. Notably, a clear 4–5 cm^{-1} upshift of the main negative band at 1700 cm^{-1} was observed upon the double mutation. All of the other

double-substitution mutants showed FTIR difference spectra very similar to that of WT. The $P700^+$ EPR linewidth as well as the visible $P700^+$/P700 difference spectrum were also found to be specifically perturbed in the PsaA–His676/PsaB–His656 double Gln mutant [22]. Single His-to-Gln mutations were introduced at each one of these two sites and the change at PsaA–His676 was found to be responsible for most of the effect on the FTIR difference spectrum of the PsaA–His676/PsaB–His656 double Gln mutant [22]. Finally, an additional single mutant in which PsaA–His676 was changed to a Ser side chain revealed changes of the FTIR difference spectrum very similar to those exhibited by the mutant bearing a Gln at the same site (J. Breton, W. Leibl, A. Weber, unpublished).

On the basis of the comparison with the cation-minus-neutral FTIR difference spectrum of Chl_a in organic solvents (Fig. 1), the 1700 cm^{-1} band in the $P700^+$/P700 FTIR difference spectrum has been assigned to the 9-keto C=O group of at least one of the two Chl_a molecules that constitute P700 [9]. The high value of this frequency shows that such group(s) must be free from hydrogen bonding interaction with the protein. Thus, the upshift in frequency of the 1700 cm^{-1} band upon change of PsaA–His676 to Gln [22] cannot be due to the loss of an hydrogen bond to a 9-keto group and is consistent with a repositioning of the whole P700 dimer upon mutation of one axial ligand. Such a change in the position of the dimer in the protein cavity, by altering the constraints on the macrocycle as well as the conformation and/or local electrostatic of the substituents on ring V for each member of the dimer, is liable to induce frequency shifts of these peripheral groups. The conclusion that PsaA–His676 and PsaB–His656 are the axial ligands to the Chl of P700 is further supported by the strong perturbation of the light-induced $P700^+$/P700 FTIR difference spectrum of a mutant in which PsaB–His656 is changed for a Leu residue [23].

2.4. Isotope labeling studies

The effect of global isotope labeling with ^{15}N or with ^2H on the $P700^+$/P700 FTIR difference spectra recorded at 90 K has been recently reinvestigated in PSI preparations from *Synechocystis* PCC 6803 [19]. This approach was used to discriminate the C=O vibrations of the Chl from those of the protein in the region 1800–1600 cm^{-1}. The rationale is that ^{15}N labeling does not affect the C=O vibrations of the Chl but induces a small downshift of the peptide C=O while ^2H labeling induces a small frequency downshift of the C=O vibrations of both the Chl and the peptide. Of the three main negative bands observed at 90 K in the $P700^+$/P700 FTIR difference spectrum at 1697, 1668, and 1637 cm^{-1} (Fig. 2b) that are possible candidates for 9-keto groups of the P700 Chl, only the one at 1668 cm^{-1} was affected in a manner consistent with a protein C=O, while the two others (1697 and 1637 cm^{-1}) were behaving more like Chl 9-keto C=O groups. Furthermore, the two negative bands at 1749 and 1733 cm^{-1} could be assigned to 10a-ester C=O vibrations from the P700 Chl on the basis of their 5 cm^{-1} isotopic shift upon ^2H labeling, which is equivalent to that observed for the same group in isolated Chl_a. Similarly, the isotope effects observed on the positive bands at 1754, 1740, 1717, and 1656 cm^{-1} allowed their assignment to the upshifted vibrations in $P700^+$ associated with the four negative Chl C=O bands of P700 at 1749, 1733, 1697, and 1637 cm^{-1}, respectively [19]. The assignments of these carbonyls of the Chl of P700 are summarized in Table 1.

Recently, a selective labeling strategy has been applied to the $P700^+$/P700 FTIR difference spectrum of PSI from *Synechocystis* PCC 6803 whereby the meth-

Table 1
Assignment of carbonyl stretching frequencies (cm^{-1}) of the two chlorophylls of P700 in *Synechocystis* SPP 6803 at 90 K

	Carbonyl	P700	$P700^+$	$^3P700$
Chl P_1 (eC-A_1)	10a-ester	1733	~1740	~1728
	9-keto	1637	1656	1594
Chl P_2 (eC-B_1)	10a-ester	1749	1754	
	9-keto	1697	1717	

The two chlorophyll molecules constituting P700 are denoted P_1, P_2 and eC-A_1, eC-B_1 in [19,46], respectively.

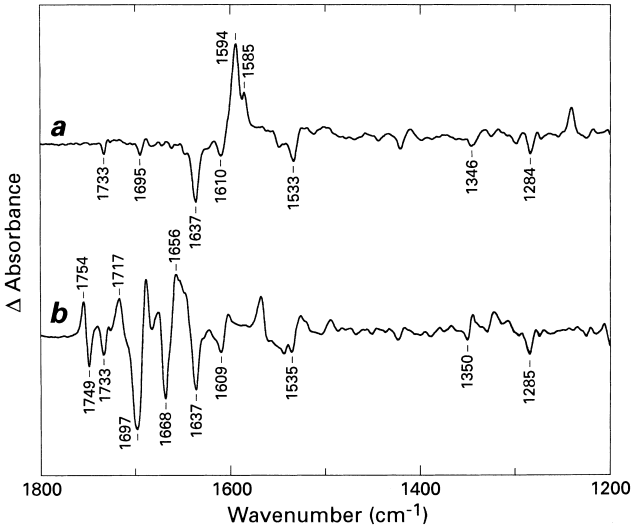

Fig. 2. Light-induced FTIR difference spectra of PSI particles from *Synechocystis* PCC 6803 at 90 K. (a) ^{3}P700/P700 triplet-minus-singlet spectrum on FeS-depleted PSI. (b) P700$^+$/P700 spectrum on native PSI. Peak-to-peak amplitudes are 4×10^{-4} and 6×10^{-4} absorbance units in a and b, respectively.

yl attached to the 10a-ester C=O of the Chl is labeled upon feeding ^{2}H-labeled methionine to this organism [24]. Although intrinsically more specific than our global ^{2}H labeling [19], this selective approach leads to a ^{1}H-minus-^{2}H double-difference spectrum that is very close to ours in the range 1760–1710 cm^{-1}. Notably, positive bands at 1754, 1745, 1730, and 1720 cm^{-1} and negative bands at 1750, 1737, 1726, and 1714 cm^{-1} in [24] are located within less than 2–3 cm^{-1} of analogous peaks in [19]. Moreover, the small shifts in frequency that can be observed between the spectra in these studies are essentially due to the difference in temperature in the two experiments, i.e., 264 K in [24] and 90 K in [19] (J. Breton, unpublished). This similarity is to be expected as in both experiments the methyl of the 10a-carbomethoxy group is labeled with ^{2}H. We had assigned the two main differential features at 1754/1749 and 1740/1733 cm^{-1} in the P700$^+$/P700 difference spectrum of the unlabeled sample at 90 K to the free and hydrogen-bonded 10a-ester C=O vibrations from the two Chl in P700 [19]. We concur with the authors in [24] that the small positive peak around 1730 cm^{-1} in the P700$^+$/P700 difference spectrum of the unlabeled sample probably reflects an heterogeneity of the conformation of one of the 10a-ester C=O groups. However, we propose that the small differential signal that they observe under the 1717 cm^{-1} positive peak of the P700$^+$/P700 difference spectrum of the unlabeled sample is not to be assigned to an additional population of 10a-ester C=O as discussed in [24] but is rather to be attributed to the 9-keto C=O of one of the Chl in P700$^+$ that is affected by the ^{2}H labeling of the 10a-carbomethoxy group through vibrational coupling. This proposal relies on the observation that ^{2}H labeling of the 10a-carbomethoxy group and of the hydrogen atom at C_{10} induces a 3 cm^{-1} downshift of the 9-keto frequency in isolated Chl$_a$ [19]. The latter phenomenon could also help rationalize the unexplained weak isotope effects on bands underlying the main 1697 cm^{-1} band reported in [24].

2.5. Comparison of P700$^+$/P700 and ^{3}P700/P700 FTIR difference spectra

In a light-induced FTIR difference spectrum of the photooxidation of P, the identification of the C=O vibrations from the primary donor (B)Chl(s) is hampered by the likely possibility that the positive charge on P$^+$ and the negative charge on the reduced electron acceptor could perturb the protein C=O vibrations that are in the vicinity of these charges and that absorb in the same spectral range. This difficulty does not exist when the triplet state of P is generated owing to the electroneutral character of the triplet. Furthermore, the mere comparison of the P$^+$/P and ^{3}P/P difference spectra offers the interesting possibility of identifying the C=O vibrations of the neutral (B)Chl(s) of P as the common negative bands in the carbonyl frequency range of the two spectra. This strategy was first applied to the primary donor BChls of P870 in *Rb. sphaeroides* where common negative bands at ~1682 and 1692 cm^{-1} could be identified as the 9-keto C=O of the two BChl molecules constituting P870 [25].

The ^{3}P700/P700 difference spectrum generated at 90 K on PSI particles from *Synechocystis* PCC 6803 that had been depleted of the FeS centers F_A, F_B, and F_X (Fig. 2a) exhibits a main negative band at 1637 cm^{-1} associated to a positive band at 1594 cm^{-1} [19]. These two bands can be assigned to the 9-keto C=O of a Chl$_a$ in vivo on the basis of the comparable frequency downshift observed for the 9-keto C=O upon triplet formation of Chl$_a$ in the

solvent THF [19]. The frequency of the negative band at 1637 cm^{-1} in the ^{3}P700/P700 spectrum (Fig. 2a) closely matching that of a negative band in the P700$^+$/P700 difference spectrum (Fig. 2b), it has been concluded that this band can be attributed to the 9-keto C=O mode of one of the Chl_a that constitutes P700 [19] and that is denoted P_1 in the following (Fig. 3). The ^{3}P700/P700 difference spectrum also shows a small negative band at 1733 cm^{-1} matching a negative band at the same frequency in the P700$^+$/P700 spectrum (Fig. 2) which is thus assigned to the 10a-ester C=O of P_1. For this Chl molecule of P700, the downshifted IR frequencies compared to isolated Chl_a in THF show that both the 9-keto and the 10a-ester C=O groups are hydrogen bonded. The second Chl_a molecule of P700, denoted P_2, with its 9-keto and 10a-ester C=O vibrations at 1697 and 1749 cm^{-1}, respectively, is free from interactions with the protein. While P_2 is essentially unaffected by the formation of ^{3}P700, it makes a large contribution to the P700$^+$/P700 difference spectrum. These assignments, summarized in Table 1, have been further reinforced by analyzing the effect of global isotope labeling on the ^{3}P700/P700 difference spectrum [19]. The conclusion that the triplet state in ^{3}P700 is entirely localized on a single Chl_a molecule is consistent with the D and E values found by EPR although a dimeric state with parallel planes of the Chl_a molecules could not be excluded by the magnetic resonance studies [26,27].

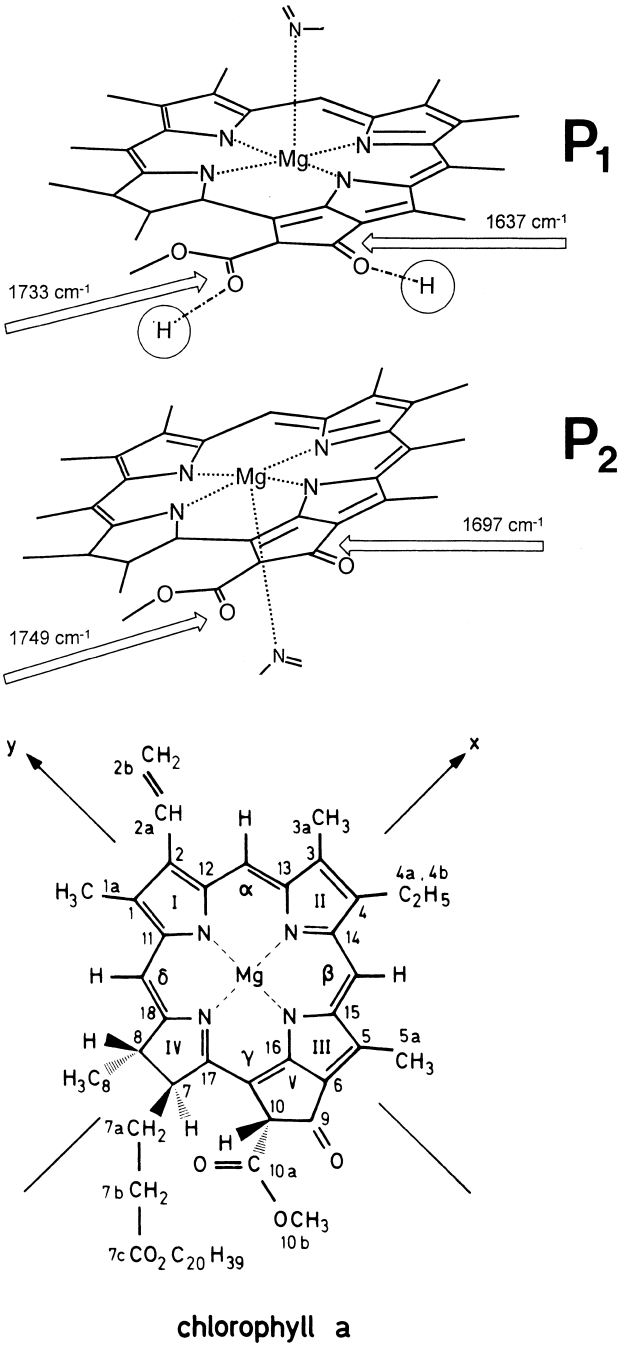

2.6. *Mid-IR electronic transition of P700$^+$. Charge repartition in P700$^+$*

The presence of an electronic mid-IR transition peaking around 3300–3100 cm^{-1} implies that the hole in P700$^+$ is delocalized over more than one Chl_a molecule [19]. From the global isotopic labeling studies, the comparison with model compounds, and the analysis of the FTIR spectrum of ^{3}P700 formation, it has been concluded that the positive charge in P700$^+$ is shared amongst the two halves of the dimer

←

Fig. 3. Schematic representation of the bonding interactions of the two chlorophyll molecules in P700 as derived from FTIR spectroscopy. The triplet state of P700 is fully localized on a chlorophyll, denoted P_1, with strong hydrogen bonds to both the 9-keto and 10a-ester C=O groups. For the second chlorophyll, denoted P_2, these carbonyls are free from hydrogen bonding interaction. For the Mg atom of each chlorophyll, a fifth axial ligand is provided by the side chains of histidine PsaA676 or PsaB656 (*Chlamydomonas reinhardtii* sequence numbering). The IR frequency of the four carbonyls are indicated with arrows for the neutral chlorophylls in P700. The positive charge in P700$^+$ is shared between P_1 and P_2 with a distribution ranging from 1:1 to 2:1 (in favor of P_2). The structural formula of Chl_a is given in the bottom part of the figure.

as discussed in [19]. For PSI particles from *Synechocystis* PCC 6803 at 90 K, the C=O groups of P_1 absorb at 1733 and 1637 cm^{-1} while those of P_2 are found at 1749 and 1697 cm^{-1}. Very similar characteristics are observed at higher temperatures and for PSI particles from other organisms (Fig. 4). The extent of perturbation (as estimated by the frequency upshift) upon $P700^+$ formation is approximately the same for the 9-keto of P_1 (19 cm^{-1}) and of P_2 (20 cm^{-1}) and close to that (25 cm^{-1}) observed for this group upon Chl_a^+ formation in THF. The differential features associated with the 10a-ester C=O vibrations of P_1 and P_2 are also quite equivalent (Fig. 4). Insofar as the 9-keto and the 10a-ester C=O vibrations are both coupled to the ring V, which itself is fully conjugated to the Chl_a macrocycle, it was further concluded that the charge is shared roughly equally between the two Chl_a molecules of P700 with a ratio ranging between 1:1 and 2:1 in favor of P_2 [19]. Although this proposal of a strong delocalization of the hole over the two halves of the $P700^+$ dimer agrees well with the early interpretations of EPR and ENDOR data [28,29] it is at variance with the more recent conclusions derived from advanced magnetic resonance studies pointing to a predominant or even complete localization of the charge on a single Chl molecule [30–34]. It has to be recognized, however, that the charge and spin distribution is not necessarily the same. The hyperfine coupling constants measured by EPR techniques reflect the polarized spin distribution which could lead to a stronger asymmetry of the distribution of the spin than of the charge. Furthermore, the effect of the local environment, which is likely to play some role in P700, has been shown to influence the spin density distribution of isolated Chl_a^+ [34]. Both FTIR and EPR techniques probe the distribution at only a few positions of the system as the latter samples the excess spin mainly on three methyl groups attached to the Chl macrocycle while the former measures the change of bond order of two C=O groups that are partially (10a-ester) or fully (9-keto) conjugated to the macrocycle. Although some variations in the exact value of the spin or charge distribution estimated by the two different techniques are thus to be expected, it is still not possible to reconcile the evidence of strong charge delocalization on both Chl deduced from FTIR measurements [19] and the conclusion

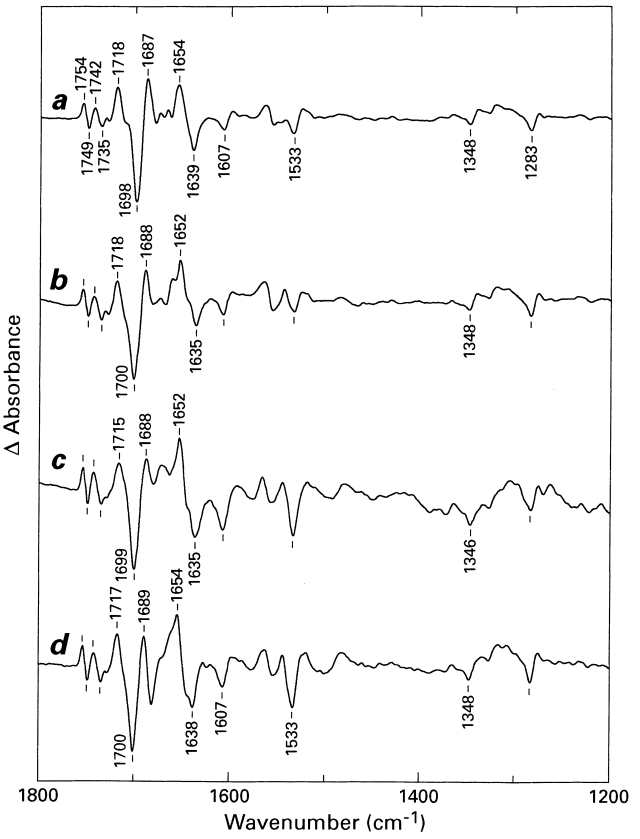

Fig. 4. Light-induced $P700^+$/P700 FTIR difference spectra at 5°C of the photooxidation of PSI particles from (a) *Synechocystis* PCC 6803 as a dry film and from (b) *Synechocystis elongatus*, (c) *Chlamydomonas reinhardti*, and (d) spinach as wet samples. Peak-to-peak amplitudes are 2×10^{-3}, 7×10^{-4}, 3×10^{-4}, and 4×10^{-4} absorbance units in a, b, c, and d, respectively.

derived from EPR that the charge in $P700^+$ is essentially localized on only one half of P700 while the other Chl carries no or very little (less than 15%) spin density [34].

2.7. Structure of P700. Comparison with X-ray data

The evidence coming from the FTIR spectra that two Chl_a molecules constitute the P700 special pair of PSI agrees with previous spectroscopic observations [35–40] as well as with the crystallographic model of PSI at 4 Å resolution that shows two stacked macrocycles with their plane parallel to the membrane normal [1,2]. This geometry is similar to that of the special pair in purple bacteria. In both the $^3P700$/P700 and the $P700^+$/P700 difference spectra, marker bands at $\sim$1610 and 1535 cm^{-1} are typical

for 5-coordination of the central Mg atom [41]. The absence of 6-coordinated Mg marker bands at around 1600 and 1515 cm^{-1} in the $P700^+$/P700 spectrum indicates that each of the Chl_a molecules in P700 has only one axial ligand. These ligands have been previously identified as PsaA–His676 and PsaB–His656 (*Chlamydomonas* sequence numbering) [22]. The IR frequencies of 1749 and 1697 cm^{-1} found for the 10a-ester and 9-keto C=O groups of P_2, respectively, are typical for free carbonyls. On the other hand, the band of P_1 at 1733 cm^{-1} corresponds to a bound 10a-ester C=O, while that at 1637 cm^{-1} is indicative of an unusually large perturbation of a 9-keto C=O group such as that induced by a very strong hydrogen bond [42,43].

One of the unique properties of the P700 special pair deals with its redox midpoint potential that is about 400 mV lower than Chl_a in vitro. In contrast, the primary donor of purple bacteria has a midpoint potential only about 200 mV less positive than $BChl_a$ in solution and P680 is some hundred mV more positive than Chl_a in vitro. In order to rationalize the unusual redox potential and magnetic resonance properties of $P700^+$, a monomeric Chl_a enol has been put forward as an alternative model to the P700 dimer [11,44]. Enolization of the ring V β-keto ester of Chl_a results in a very different π electronic structure of the macrocycle. The frequency of 1637 cm^{-1} observed for the 9-keto C=O group of P_1 is consistent with at least a partial enolization of ring V. In the case of purple bacteria, specific alterations of the oxidation potential of P870 by interaction with the protein scaffold have been characterized in mutant RCs of *Rb. sphaeroides*. In particular, introduction of hydrogen bonds to the 9-keto or 2a-acetyl C=O groups of $BChl_a$ leads to an increase of the redox potential of P870 by 60–125 mV per hydrogen bond [45]. Thus, the unusual strength of the hydrogen bond that is responsible for the observed frequency of 1637 cm^{-1} of the 9-keto C=O group of P_1 cannot be related directly to the low oxidation potential of P700. It is possible that the hydrogen bonds control only indirectly the redox potential of P, e.g., by influencing the conformation of the macrocycle which could be a main determinant of the midpoint potential.

Very recently, a crystallographic structure of PSI at 2.5 Å resolution that bears on several issues of the organization of the two Chl molecules in P700 as deduced from FTIR difference spectroscopy has been reported [46]. Notably, the conclusion that the histidine side chains of PsaA–His676 and PsaB–His656 (*Chlamydomonas* sequence numbering) are the axial ligands to the Chl of P700 [22] has been confirmed. Furthermore, the strong inequivalence of the hydrogen bonding pattern of the carbonyl groups of the two Chl molecules in P700, that has been initially described in [19], is also apparent in the new crystallographic structure [46]. The latter shows one Chl molecule having no hydrogen bond while the other has three including those at the 9-keto and 10a-carbomethoxy positions determined in the FTIR study [19]. Additional important information that is provided by the new crystallographic study includes the determination that the strongly hydrogen bonded Chl half of P700, denoted eC-A_1, is actually a $Chl_{a'}$ molecule (epimer of Chl_a at C_{10} [47]; the stereochemistry of Chl_a at C_{10} is shown in the bottom of Fig. 3). In the structural model [46], the 9-keto of eC-A_1 is hydrogen bonded to a Thr side chain and the 10a-carbomethoxy group is hydrogen bonded to a water molecule interacting with the same Thr side chain as well as with several other residues. It should be noted that the present description of this water donating a hydrogen bond to the methoxy oxygen atom of the 10a-carbomethoxy group [46] differs from that deduced from the FTIR study that shows a perturbation of the IR frequency of the C=O double bond of the 10a-carbomethoxy ester group [19]. The third hydrogen bond, located between the 7c-ester C=O and a Tyr residue, was not detected by FTIR, an observation essentially consistent with the lack of conjugation with the Chl macrocycle of this ester group [8,9]. The central Mg atom of eC-A_1 is liganded to the PsaA polypeptide. On the other hand, the Chl_a molecule liganded to the PsaB polypeptide, denoted eC-B_1, is free from hydrogen bond interaction. It is thus straightforward to equate eC-A_1 and eC-B_1 with P_1 and P_2 in our model (Fig. 3), respectively (Table 1). Therefore the new data on the axial Mg ligands and on the bonding pattern of the carbonyls of P700 obtained from X-ray crystallography are in excellent agreement with the conclusions previously derived from FTIR difference spectroscopy [19]. Furthermore, the present description of the crystallographic structure [46] provides some clues

concerning the cause of the unusually large magnitude of the frequency downshift of the 9-keto of eC-A_1. This vibration is shifted by about 60 cm^{-1} compared to that of eC-B_1 and it is unlikely that the hydrogen bond to a Thr side chain alone could lead to such an unusually strong downshift. However, the crystallographic structure proposes that this Thr side chain itself is in hydrogen bond interaction with a special water molecule that is at the center of a web of hydrogen bonds involving the carbomethoxy group of eC-A_1 as well as several other amino acid side chains. It is thus conceivable that the special geometry of this network of hydrogen bonds makes the hydrogen atom of the Thr side chain sufficiently acidic to lead to the large downshift of the vibration of the 9-keto of eC-A_1. A comparable interpretation has been proposed for Chl_a-water aggregates in which coordination of the Mg atom of the Chl by the oxygen of a water molecule makes one of the hydrogen atom of the water sufficiently acidic to downshift to 1640 cm^{-1} the 9-keto of the Chl [42,43].

Our conclusions from FTIR spectroscopy that the ^{3}P700 triplet is fully localized on the Chl denoted eC-A_1 while the charge in $P700^+$ is shared between eC-A_1 and eC-B_1 [19] are at odds with the interpretations proposed in a recent study of the effect of substitution of the histidine axial ligands of P700 on the redox potential of P^+/P, the ENDOR spectra of $P700^+$, the $P700^+/P700$ optical spectra, and the triplet-minus-singlet electronic absorption measured by ADMR [48]. In the latter study, conducted at 1.8 K, it was concluded that the triplet character in ^{3}P700 is mainly localized on eC-B_1, i.e., the same Chl molecule that, according to EPR measurements, also carries the positive charge in $P700^+$. This strong discrepancy is not likely to be due to a difference in the temperature at which the two experiments are conducted as both the $P700^+/P700$ and the ^{3}P700/P700 FTIR difference spectra are almost unchanged when the temperature is lowered from 90 to 10 K (J. Breton, W. Leibl, unpublished). Such a large disagreement cannot be blamed on some unusual vibrational property of porphyrin as changes of bond order occurring upon triplet or cation formation for (B)Chl_a in solution have been extensively documented using both FTIR [6,8,9,19,49,50] and Raman spectroscopies [10,12,51–53]. In addition, the suggestion was put forward in [48] that the FTIR data on $P700^+/P700$ in [19] could be explained by considering that the unpaired electron localized on one of the Chl in $P700^+$ electrostatically influences the frequency of the carbonyl of the neighboring neutral Chl. This interpretation appears unlikely as the frequency upshift observed upon $P700^+$ formation is the same for the 9-keto vibration of eC-A_1 (19 cm^{-1}) and of eC-B_1 (20 cm^{-1}) and is close to that (25 cm^{-1}) observed for isolated Chl_a in THF [9]. New FTIR experiments involving *Synechocystis* PCC 6803 mutants are currently being performed to help settle the discrepancies between the results obtained by the FTIR and EPR techniques.

2.8. Response of the protein

The available FTIR data provide indications that no large conformational changes of the protein occur upon charge separation at the level of P700. A 1674(+)/1668(−) cm^{-1} differential signal observed upon P700 photooxidation at 90 K exhibits isotopic shifts compatible with a small contribution from amide I peptide C=O group(s) [19]. Similarly, a 1567(+)/1558(−) cm^{-1} differential signal within the amide II band, that shifts by 15 cm^{-1} upon global ^{15}N labeling, is clearly due to some change of conformation at the level of a peptide NH bending mode. The signal in the amide I region is somewhat reduced at ambient temperatures and exhibits variability from species to species (Fig. 4). It should be noticed, however, that the difference spectra contains also contributions from the FeS electron acceptors and that the small conformational changes described above could originate from the change of redox state of these cofactors. Comparison of FTIR difference spectra of P700 photooxidation in PSI samples measured in the presence or the absence of electron acceptors such as methyl viologen or ferricyanide has revealed clear spectral signatures of the $F_{A,B}$ iron-sulfur centers which remain to be analyzed in detail (W. Leibl, J. Breton, unpublished).

The lack of an effect of $^1H/^2H$ exchange on the bands above 1700 cm^{-1} [16,19] shows the absence of contributions from exchangeable protonated carboxylic groups. On the other hand, contributions from histidine side chains have been detected using PSI particles prepared from *Synechocystis* PCC 6803

selectively labeled with [^{13}C]histidine (J. Breton, B.A. Diner, unpublished).

3. FTIR spectroscopy of primary donors in other type I reaction centers

3.1. Green sulfur bacteria

The light-induced FTIR difference spectra of P840 photooxidation reported for chlorosome-depleted membranes of *Chlorobium limicola* [17] and for the reaction center complex of *C. tepidum* [54] are highly comparable. In both cases a prominent mid-IR electronic transition peaking around 2500 cm^{-1} together with well-developed positive bands at ~1465 and 1280 cm^{-1} were observed. These features closely resemble those previously observed in the P870^{+}/P870 FTIR difference spectrum of *Rb. sphaeroides* indicating a comparable organization of the BChl$_a$ molecules in P840 and P870 and a similar charge repartition in the two oxidized special pairs. However, the quality of the spectra in these initial studies was poor in the region above 3000 cm^{-1} which is always difficult to measure owing to the strong background absorption of the OH stretching vibration of water and the low sensitivity of the commonly used MCT detectors. This is unfortunate as it has been recently proposed that the profile of the mid-IR electronic transition in this frequency range was critical for assessing the extent of coupling between the two halves of P^{+} [55]. Therefore, we have recently reinvestigated this question using purified reaction centers complexes from *C. tepidum* (in collaboration with H. Sakurai) and an optimized detection set-up [56]. The result is illustrated in Fig. 5 which compares the P840^{+}/P840 and P870^{+}/P870 FTIR difference spectra and shows very similar band profiles for the electronic transitions of these two classes of photosynthetic bacteria. Thus, it can be stressed that the charge repartition and the extent of coupling should be very close in P840^{+} and P870^{+}. The intense positive bands at ~1480 and 1295 cm^{-1} in *Rb. sphaeroides* have been attributed to phase-phonon bands corresponding to specific modes of the BChl$_a$ macrocycle as the hole moves back and forth between the two halves of P^{+} [55]. The bands at ~1465 and 1280, 1130, and 1008 cm^{-1} in *C. tepidum* most probably have the same origin.

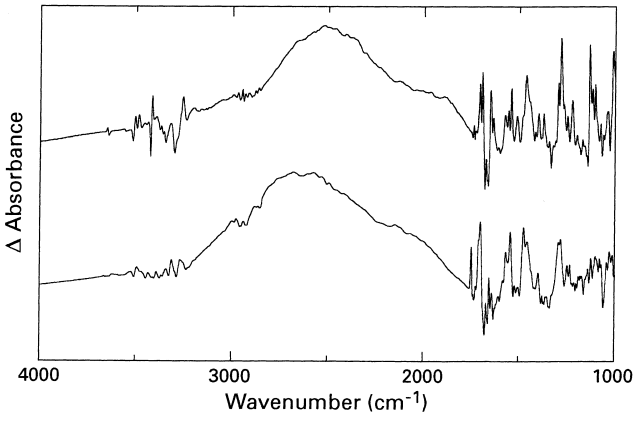

Fig. 5. Light-induced FTIR difference spectra at 240 K of the photooxidation of the primary electron donor in reaction centers from *Chlorobium tepidum* (top) and from *Rhodobacter sphaeroides* (bottom). Peak-to-peak amplitudes are 4×10^{-4} and 9×10^{-3} absorbance units for top and bottom, respectively.

In the spectral range where the 9-keto C=O groups of BChl$_a$ are expected to absorb, the P840^{+}/P840 FTIR difference spectrum shows a splitting of the positive band at 1707 and 1694 cm^{-1} with a single main negative band at 1684 cm^{-1}. This point, which is interesting in view of the proposed homodimeric nature of the RC of *C. tepidum*, the core of which is thought to be made of two identical polypeptides [57,58], has been discussed in terms of various models for the symmetry of the P840 dimer [54]. An indication of the presence of some bands belonging to the iron-sulfur center in the spectral range 1670–1620 cm^{-1} has been provided in the case of *C. tepidum* [54].

3.2. Heliobacteria

The light-induced FTIR difference spectra of P798 photooxidation reported for membranes of *Heliobacillus chlorum* [17] and for membranes or reaction center complexes of *H. modesticaldum* [59] are highly comparable. They both show a mid-IR electronic transition peaking around 2050–2100 cm^{-1} and with a characteristic skewed shape highly reminiscent of the mid-IR electronic transition associated with P680^{+} of PSII (Fig. 6; see also [60]). Several positive bands, most notably those at 1300 and 1110 cm^{-1}, are likely to originate from the intensification of por-

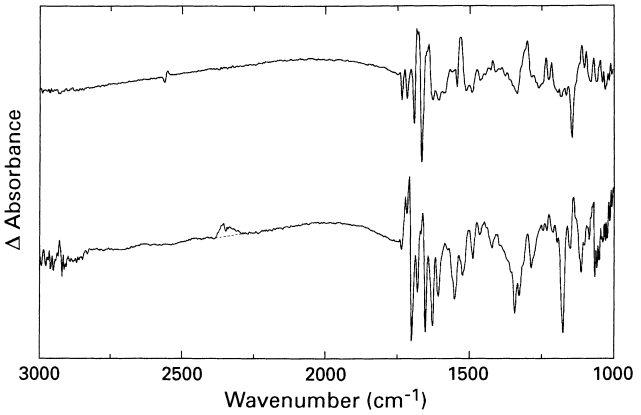

Fig. 6. Light-induced FTIR difference spectra at 240 K of the photooxidation of the primary electron donor in reaction centers from *Heliobacillus mobilis* (top) and from PSII of spinach (bottom). Peak-to-peak amplitudes are 3×10^{-4} and 4×10^{-4} absorbance units for top and bottom, respectively.

phyrin modes in the dimeric state of $P798^+$ giving rise to phase-phonon bands [59].

In the spectral range where the C=O groups of $BChl_g$ are expected to absorb, the $P798^+$/P798 FTIR difference spectrum shows a single differential signal positive at 1702 cm^{-1} and negative at 1693 cm^{-1} which has been tentatively assigned to the upshift upon cation formation of the 9-keto group(s) of the homodimeric P798 while two differential signals at 1741/1737 and 1725/1718 cm^{-1} are more probably related to the 10a-ester C=O [59]. A small differential feature at 2550/2560 cm^{-1}, which is insensitive to $^1H/^2H$ exchange but can be labeled upon growing the bacteria in ^2H_2O, has been convincingly assigned to a cysteine S–H mode engaged in a strong hydrogen bond, and this SH group is proposed to be closely associated with P798 [59].

4. Conclusion and outlook

Concerning the general organization of P700, there is good agreement between the conclusions derived from light-induced FTIR difference spectroscopy and the most recent results from the crystallographic studies on *Synechococcus* [46]. This allows interesting functional implications to be derived such as the conclusion that the $^3P700$ triplet state at low temperature is localized on the $Chl_{a'}$ molecule that also exhibits one unusually strong hydrogen bond. In contrast, the hole in $P700^+$ is distributed over the two halves of P700 with a repartition of charge varying between 1:1 and 2:1 (in favor of the eC-B_1 Chl_a molecule) both at room and cryogenic temperatures. It will be of interest to examine the further refinements of the high-resolution crystallographic model and the results of the studies by FTIR and magnetic resonance spectroscopy to try to relate the strong discrepancy between the conclusions derived from the latter two spectroscopic techniques on both the localization of the $^3P700$ state and the charge repartition in the $P700^+$ state to a difference in, e.g., the conformation of the macrocycles of the Chl molecules or the effect of the local environment of the methyl and carbonyl groups of P700.

For the primary electron donors of the green sulfur bacteria and of the heliobacteria, the interpretation of the results of FTIR spectroscopy is far less advanced than in the case of PSI. Some evidence for a dimeric primary donor, notably in the cationic state of P, has been provided. The generation of triplet-minus-singlet FTIR difference spectra would be of great help to assign the IR bands of the carbonyls of the chlorophylls constituting the primary electron donors.

Acknowledgements

The author thanks Eliane Nabedryk and Winfried Leibl for extensive discussions of the results and for a critical reading of the manuscript. Uhlrich Mülhenhoff, Kevin Redding, and Hidehiro Sakurai are greatly acknowledged for their kind gift of reaction center complexes of *Synechococcus elongatus*, *Chlamydomonas reinhardtii*, and *Chlorobium tepidum*, respectively. The author is most thankful to Norbert Krauss for providing unpublished information on the crystallographic structure of P700.

References

[1] N. Krauss, W.-D. Schubert, O. Klukas, P. Fromme, H.T. Witt, W. Saenger, Nat. Struct. Biol. 3 (1996) 965–973.
[2] W.-D. Schubert, O. Klukas, N. Krauss, W. Saenger, P. Fromme, H.T. Witt, J. Mol. Biol. 272 (1997) 741–769.

[3] B.A. Tavitian, E. Nabedryk, W. Mäntele, J. Breton, FEBS Lett. 201 (1986) 151–157.
[4] W. Mäntele, E. Nabedryk, B.A. Tavitian, W. Kreutz, J. Breton, FEBS Lett. 187 (1985) 227–232.
[5] B.A. Tavitian, Thesis, Université P. et M. Curie, Paris VI, 1987.
[6] W. Mäntele, A. Wollenweber, F. Rashwan, J. Heinze, E. Nabedryk, G. Berger, J. Breton, Photochem. Photobiol. 47 (1988) 451–455.
[7] B.A. Tavitian, E. Nabedryk, A. Wollenweber, W. Mäntele, J. Breton, in: E.D. Schmid, F.W. Schneider, F. Siebert (Eds.), Spectroscopy of Biological Molecules, New Advances, Wiley, New York, 1988, pp. 297–300.
[8] M. Leonhard, A. Wollenweber, G. Berger, J. Kléo, E. Nabedryk, J. Breton, W. Mäntele, in: J. Barber (Ed.), Techniques and New Developments in Photosynthesis Research, Plenum Press, New York, 1989, pp. 115–118.
[9] E. Nabedryk, M. Leonhard, W. Mäntele, J. Breton, Biochemistry 29 (1990) 3242–3247.
[10] R.L. Heald, P.M. Callahan, T.M. Cotton, J. Phys. Chem. 92 (1988) 4820–4824.
[11] M.R. Wasielewski, J.R. Norris, L.L. Shipman, C.-P. Lin, W.A. Svec, Proc. Natl. Acad. Sci. USA 78 (1981) 2957–2961.
[12] R.L. Heald, T.M. Cotton, J. Phys. Chem. 94 (1990) 3968–3975.
[13] G.M. MacDonald, K.A. Bixby, B.A. Barry, Proc. Natl. Acad. Sci. USA 90 (1993) 11024–11028.
[14] E. Nabedryk, in: H.H. Mantsch, D. Chapman (Eds.), Infrared Spectroscopy of Biological Molecules, Wiley–Liss, New York, 1996, pp. 39–81.
[15] E. Hamacher, J. Kruip, M. Rögner, W. Mäntele, in: T. Theophanides, J. Anastassopoulou, N. Fotopoulos (Eds.), Fifth Internat. Conf. on the Spectroscopy of Biological Molecules, Kluwer Academic Publishers, Dordrecht, 1993, pp. 163–164.
[16] E. Hamacher, J. Kruip, M. Rögner, W. Mäntele, Spectrochim. Acta A 52 (1996) 107–121.
[17] E. Nabedryk, W. Leibl, J. Breton, Photosynth. Res. 48 (1996) 301–308.
[18] J. Breton, E. Nabedryk, W.W. Parson, Biochemistry 31 (1992) 7503–7510.
[19] J. Breton, E. Nabedryk, W. Leibl, Biochemistry 38 (1999) 11585–11592.
[20] L. Cui, S.E. Bingham, M. Kuhn, H. Kass, W. Lubitz, A.N. Weber, Biochemistry 34 (1992) 1549–1558.
[21] A.N. Weber, H. Su, S.E. Bingham, H. Kass, L. Krabben, M. Kuhn, R. Jordan, E. Schlodder, W. Lubitz, Biochemistry 35 (1996) 12857–12863.
[22] K. Redding, F. MacMillan, W. Leibl, K. Brettel, J. Hanley, A.W. Rutherford, J. Breton, J.-D. Rochaix, EMBO J. 17 (1998) 50–60.
[23] W. Leibl, K. Brettel, E. Nabedryk, J. Breton, J.-D. Rochaix, K. Redding, in: G. Garab (Ed.), Photosynthesis: Mechanisms and Effects, Vol. 1, Kluwer Academic Publishers, Dordrecht, 1998, pp. 595–598.
[24] S. Kim, B.A. Barry, J. Am. Chem. Soc. 122 (2000) 4980–4981.
[25] J. Breton, E. Nabedryk, Chem. Phys. Lett. 213 (1993) 571–575.
[26] H.A. Frank, M.B. McLean, K. Sauer, Proc. Natl. Acad. Sci. USA 76 (1979) 5124–5128.
[27] A.W. Rutherford, P. Sétif, Biochim. Biophys. Acta 1019 (1990) 128–132.
[28] J.R. Norris, R.A. Uphaus, H.L. Crespi, J.J. Katz, Proc. Natl. Acad. Sci. USA 68 (1971) 625–628.
[29] J.R. Norris, H. Scheer, M.E. Druyan, J.J. Katz, Proc. Natl. Acad. Sci. USA 71 (1974) 4897–4900.
[30] I.H. Davis, P. Heathcote, D.J. MacLachlan, M.C.W. Evans, Biochim. Biophys. Acta 1143 (1993) 183–189.
[31] S.E.J. Rigby, J.H.A. Nugent, P.J. O'Malley, Biochemistry 33 (1994) 10043–10050.
[32] H. Käss, P. Fromme, W. Lubitz, Chem. Phys. Lett. 257 (1996) 197–206.
[33] M. Mac, N.R. Bowlby, G.T. Babcock, J. McCracken, J. Am. Chem. Soc. 120 (1998) 13215–13223.
[34] H. Käss, P. Fromme, H.T. Witt, W. Lubitz, J. Phys. Chem. B 105 (2001) 1225–1239.
[35] K.D. Philipson, V.L. Sato, K. Sauer, Biochemistry 11 (1972) 4591–4595.
[36] J. Breton, Biochim. Biophys. Acta 459 (1977) 66–75.
[37] H. Schaffernicht, W. Junge, Photochem. Photobiol. 36 (1982) 111–115.
[38] H.J. den Blanken, A.J. Hoff, Biochim. Biophys. Acta 724 (1983) 52–61.
[39] I. Ikegami, S. Itoh, Biochim. Biophys. Acta 934 (1988) 39–46.
[40] S. Krawczyk, W. Macsymiec, FEBS Lett. 286 (1991) 110–112.
[41] M. Fujiwara, M. Tasumi, J. Phys. Chem. 90 (1986) 5646–5650.
[42] J.J. Katz, K. Ballschmiter, M. Garcia-Morin, H.H. Strain, R.A. Uphaus, Proc. Natl. Acad. Sci. USA 60 (1968) 100–107.
[43] K. Ballschmiter, J.J. Katz, J. Am. Chem. Soc. 91 (1969) 2661–2677.
[44] M.R. Wasielewski, M. Studier, J.J. Katz, Proc. Natl. Acad. Sci. USA 73 (1976) 4282–4286.
[45] J.P. Allen, J.C. Williams, J. Bioenerg. Biomembr. 27 (1995) 275–283.
[46] P. Jordan, P. Fromme, H.T. Witt, O. Klukas, W. Saenger, N. Krauss, Nature 411 (2001) 909–917.
[47] H. Maeda, T. Watanabe, M. Kobayashi, I. Ikegami, Biochim. Biophys. Acta 1099 (1992) 74–80.
[48] L. Krabben, E. Schlodder, R. Jordan, D. Carbonera, G. Giacometti, H. Lee, A.N. Webber, W. Lubitz, Biochemistry 39 (2000) 13012–13025.
[49] T. Noguchi, Y. Inoue, K. Satoh, Biochemistry 32 (1993) 7186–7195.
[50] J. Breton, E. Nabedryk, in: T. Theophanides, J. Anastassopoulou, N. Fotopoulos (Eds.), Fifth Internat. Conf. on the

Spectroscopy of Biological Molecules, Kluwer Academic Publishers, Dordrecht, 1993, pp. 309–310.
[51] T. Sashima, M. Abe, N. Kurano, S. Miyachi, Y. Koyama, J. Phys. Chem. B 102 (1998) 6903–6914.
[52] Y. Koyama, L. Limantara, Spectrochim. Acta A 54 (1998) 1127–1139.
[53] T. Sashima, L. Limantara, Y. Koyama, J. Phys. Chem. B 104 (2000) 8308–8320.
[54] T. Noguchi, N. Kusumoto, Y. Inoue, H. Sakurai, Biochemistry 35 (1996) 15428–15435.
[55] J.R. Reimers, N.S. Hush, Chem. Phys. 197 (1995) 323–332.
[56] J. Breton, E. Nabedryk, A. Clérici, Vibrat. Spectrosc. 19 (1999) 71–75.
[57] M. Büttener, D.L. Xie, H. Nelson, W. Pinther, G. Hauska, N. Nelson, Proc. Natl. Acad. Sci. USA 89 (1992) 8135–8139.
[58] U. Liebl, M. Mockensturm-Wilson, J.T. Trost, D.C. Brune, R.E. Blankenship, W. Vermaas, Proc. Natl. Acad. Sci. USA 90 (1993) 7124–7128.
[59] T. Noguchi, Y. Fukami, H. Oh-oka, Y. Inoue, Biochemistry 36 (1997) 12329–12336.
[60] T. Noguchi, T. Tomo, Y. Inoue, Biochemistry 37 (1998) 13614–13625.